Proceedings of BS2013:
13th Conference of International Building Performance Simulation Association, Chambéry, France, August 26-28

REAL-TIME OPTIMAL CONTROL OF INDOOR AIR FLOW USING REDUCED APPROACHES BASED ON POD

Alexandra Tallet[1], Cyrille Allery[1], and Francis Allard[1]
[1] LaSIE, University of La Rochelle, Av. Michel Crépeau, 17042 La Rochelle, France

ABSTRACT

The aim of this paper is to develop an optimization algorithm to control the temperature in the occupation zone, using reduced-order approaches based on POD. Two methods are employed here: an adjoint-equations method and a based response surface method. These are tested on the cases of a lid-driven cavity heated by the left and a 3D ventilated cavity, similar to a room.

NOMENCLATURE

$\mathbf{u}$	velocity field
θ	temperature field
$\mathbf{\Phi}^u$	velocity POD modes
Φ^θ	temperature POD modes
Re	Reynolds number
Pr	Prandtl number
Ri	Richardson number
ν	kinematic viscosity
D	thermal diffusivity
g	gravitational acceleration
β	volumetric thermal expansion coefficient
θ_h	hot temperature
θ_c	cold temperature
U_o	inlet velocity

INTRODUCTION

The natural ventilation systems are more and more encouraged in order to reduce the costs related to air conditioning systems during summer. Natural ventilation consists in simply opening and closing the windows and the doors of a building to induce passive cooling. Though, it is difficult to control air flow rate which explains why mechanic ventilation systems are often preferred. Here, the objective is not to develop a new system of ventilation but to use numerical simulations for real-time air flow control.
Our goal is to control the indoor air temperature, by adjusting the inlet airflow rate. To achieve it, the theory of optimal control is applied to the Fluid Mechanics equations. The numerical simulation by classical methods (DNS, LES, RANS, ...) is costly in computational time, they can not be used to active control in real time. It is therefore necessary to use reduced-order models.

The reduced-order models are here obtained by the POD (*Proper Orthogonal Decomposition*), which is the technique most commonly used. It consists in finding space basis, optimal in the sense of energy, that approximates at best on average a set of snapshots obtained experimentally or numerically of the flow (velocity, temperature, ...). Very few modes N contain almost all the energy. The Galerkin projection of the full equations (Navier-Stokes and energy equations) on the first POD modes N leads to a system of differential equations of small size N, whose unknowns are the temporal coefficients. The resolution of this dynamic system is quickly and is done in real time. The resulting system to solve is considerably smaller than the initial system (a few dozen against several hundreds of thousands) and the computational time is significantly decreased.

The works of Palomo Del Barrio et al. (2000) or Sempey et al. (2009) open the way towards the use of ROMs (*Reduced-Order Models*) in indoor air flow control. Nevertheless, they used the linear control theory whereas the governing flow equations are nonlinear. Besides, Sempey et al. (2009) monitors the air temperature by only considering the heat equation and so forgets the air flow dynamics. Ravindran (2000) applies the theory of nonlinear control to the flow around a cylinder and later, Bergmann and Cordier (2008) the flow in a channel. But, they don't consider the coupling velocity/temperature.

In this study, the theory of nonlinear optimal control is applied to Navier-Stokes and energy equations by using POD/ROMs methods. The control is performed on the boundaries conditions of velocity or/and temperature, such as :

$$u|_{\Gamma_{in}} = \alpha U_0 \quad (1)$$

$$\theta|_{\Gamma_{in}} = \sigma\theta_c \quad (2)$$

where α et σ are the control parameters.
The velocity and temperature POD bases are built here from snapshots of flows obtained with several values of boundaries conditions (typically, for several Reynolds number $Re = \frac{\alpha U_0 H}{\nu}$ and Grashof number $Gr = \frac{g\beta L^3(\sigma\theta_c - \theta_f)}{\nu^2}$).

This approach may in some cases be too costly in memory storage. Therefore, in this paper we also consider a second approach based not on the optimal control theory but on reduced response surfaces obtained by POD. These two approaches are described in the next section.

METHODOLOGY

1.1 First method

1.1.1 Model equations

An incompressible fluid flow, in a domain Ω with boundaries Γ, is considered for $t \in]0, T]$. The fluid dynamics is assumed governed by the Navier-Stokes equations and the temperature field by a convection-diffusion equation. Boussinesq approximation is performed, all the physical properties of the fluid except density in the buoyant force term are constant. The corresponding equations are:

$$\begin{cases} \nabla \cdot \mathbf{u} &= 0 \\ \dfrac{\partial \mathbf{u}}{\partial t} + [\mathbf{u} \cdot \nabla]\,\mathbf{u} &= -\dfrac{1}{\rho}\nabla p + \nu \Delta \mathbf{u} + g\beta(\theta - \theta_{ini})\mathbf{e_y} \\ \dfrac{\partial \theta}{\partial t} + [\mathbf{u} \cdot \nabla]\,\theta &= \gamma \Delta \theta \end{cases} \tag{3}$$

with the initial conditions : $\mathbf{u}(0, \mathbf{x}) = \mathbf{u_0}(\mathbf{x})$ and $\theta(0, \mathbf{x}) = \theta_0(\mathbf{x})$ and the boundary conditions which will specify later on each studied cases.

1.1.2 Fields decomposition

In the first time, $N_\alpha \times N_\sigma$ simulations are realized in order to constitute the sampling (snapshots of velocity and temperature). N_α and N_σ represent respectively the used parameters number related to the various boundaries conditions $\alpha_1 \dots \alpha_{N_\alpha}$ and $\sigma_1 \dots \sigma_{N_\sigma}$. So, each field depends on the parameters $\boldsymbol{\alpha}$ and $\boldsymbol{\sigma}$. The velocity and temperature fields are decomposed into a mean part and a fluctuating part, such as:

$$\begin{aligned} \mathbf{u}(\mathbf{x}, t, \boldsymbol{\alpha}, \boldsymbol{\sigma}) &= \bar{\mathbf{u}}(\mathbf{x}, \boldsymbol{\alpha}, \boldsymbol{\sigma}) + \mathbf{u}'(\mathbf{x}, t, \boldsymbol{\alpha}, \boldsymbol{\sigma}) \\ \theta(\mathbf{x}, t, \boldsymbol{\alpha}, \boldsymbol{\sigma}) &= \bar{\theta}(\mathbf{x}, \boldsymbol{\alpha}, \boldsymbol{\sigma}) + \theta'(\mathbf{x}, t, \boldsymbol{\alpha}, \boldsymbol{\sigma}) \end{aligned} \tag{4}$$

The POD decomposition is carried out on the fluctuating part of each field as :

$$\mathbf{u}'(\mathbf{x}, t, \boldsymbol{\alpha}, \boldsymbol{\sigma}) \approx \sum_{i=1}^{N^u} a_i(t, \boldsymbol{\alpha}, \boldsymbol{\sigma})\, \boldsymbol{\Phi}_i^u(\mathbf{x}) \tag{5}$$

$$\theta'(\mathbf{x}, t, \boldsymbol{\alpha}, \boldsymbol{\sigma}) \approx \sum_{i=1}^{N^\theta} b_i(t, \boldsymbol{\alpha}, \boldsymbol{\sigma})\, \Phi_i^\theta(\mathbf{x}) \tag{6}$$

where N^u, N^θ are respectively the kept POD number of the velocity and the temperature. $\mathbf{a}(t, \boldsymbol{\alpha}, \boldsymbol{\sigma})$ and $\mathbf{b}(t, \boldsymbol{\alpha}, \boldsymbol{\sigma})$ are the temporal coefficients, depending on the time and the parameters $\boldsymbol{\alpha}$ and $\boldsymbol{\sigma}$.

In the following, the parameters included to the POD basis are noted $\boldsymbol{\alpha}_{\text{POD}} = [\alpha^1_{\text{POD}} \ \dots \ \alpha^{N_\alpha}_{\text{POD}}]^T$ and $\boldsymbol{\sigma}_{\text{POD}} = [\sigma^1_{\text{POD}} \ \dots \ \sigma^{N\sigma}_{\text{POD}}]^T$.

1.1.3 Optimization problem

The optimization problem consists in finding state and control variables that minimize an objective functional subject to the requirement that the constraints are satisfied, Gunzburger (2003). In our case, the state variables are the velocity, temperature and pressure fields. The control parameters α and σ monitors the boundaries conditions (Eqn. 1). The objective (or cost) functional defines the goal to achieve and depends on state and control variables. Here, the aim is to minimize the difference between target and indoor temperature, which is written[1]:

$$\begin{aligned} \mathcal{J}(\theta, \alpha, \sigma) &= \frac{1}{2}\int_\Omega \int_0^T (\theta(\mathbf{x}, t) - \hat{\theta}(\mathbf{x}, t))^2 d\mathbf{x} dt \\ &+ \frac{1}{2}\int_\Omega (\,\theta(\mathbf{x})|_T - \hat{\theta}(\mathbf{x})\big|_T)^2 d\mathbf{x} \\ &+ \frac{\omega_1}{2}\alpha^2 + \frac{\omega_2}{2}\,\sigma^2 \end{aligned} \tag{7}$$

where $\hat{\theta}(\mathbf{x}, t)$ is the target temperature to reach. Finally, the constraints are the governing flow equations (Navier-Stokes equations and convection-diffusion equation). The optimization problem to solve becomes : *minimize the cost functional $\mathcal{J}$ over the control parameters α and σ, under the constraints equations (Eqn. 3).*

The resolution of this problem requires the resolution of the full equations (constraints equations, adjoint equations) many times. Then, this full optimization problem is then turned into a reduced optimization problem. Henceforth, the state variables are the temporal coefficients a_i (for $i = 1, \dots, N^u$) and b_i (for $i = 1, \dots, N^\theta$) and the objective functional[2] is expressed as:

$$\begin{aligned} \mathcal{J}(\mathbf{b}, \alpha, \sigma) &= \frac{1}{2}\sum_{i=1}^{N^\theta} \int_0^T (b_i(t) - \hat{b}_i(t))^2 \\ &+ \frac{1}{2}\sum_{i=1}^{N^\theta} (\,b_i|_T - \hat{b}_i(t)\Big|_T)^2 \\ &+ \frac{\omega_1}{2}\,\alpha^2 + \frac{\omega_2}{2}\,\sigma^2 \end{aligned} \tag{8}$$

The reduced optimization problem is thus solved according to the adjoint-based optimization method, Gunzburger (2003). In this case, the constrained optimization problem is converted into an unconstrained optimization problem, using Lagrangian multipliers (or co-state variables)

[1] ω_1 and ω_2 are penalty terms of the objective functional. Here, their value is 10^{-7}.

[2] $\hat{b}_i$ is the temporal coefficients related to the target temperature $\hat{\theta}(\mathbf{x}, t)$ to reach.

$\boldsymbol{\xi}(t)$ and $\boldsymbol{\zeta}(t)$ respectively associated at the equations (Eqn. 3) and the Lagrange functional $\mathcal{L}$, that is expressed as follows :

$$\begin{aligned}\mathcal{L}(\mathbf{a},\mathbf{b},\alpha,\sigma,\boldsymbol{\xi},\boldsymbol{\zeta}) &= \mathcal{J}(\mathbf{b},\alpha,\sigma) \\ &- \sum_{j=1}^{N^u}\int_0^T \xi_j \mathcal{N}_j(\mathbf{a},\mathbf{b},\alpha,\sigma)\,\mathrm{d}t \\ &- \sum_{j=1}^{N^\theta}\int_0^T \zeta_j\,\mathcal{M}_j(\mathbf{a},\mathbf{b},\alpha,\sigma)\,\mathrm{d}t\end{aligned} \tag{9}$$

where $\boldsymbol{\mathcal{N}}(\mathbf{a},\mathbf{b},\alpha,\sigma)=0$ and $\boldsymbol{\mathcal{M}}(\mathbf{a},\mathbf{b},\alpha,\sigma)=0$ represent respectively the reduced momentum equations and the reduced convection-diffusion equations. Their expressions are detailed in the next paragraph.

The reduced constraint equations

The decompositions (Eqns. 4 and 5) are then introduced in the full equations (Eqn. 3). Since the POD modes are divergence free by construction, the continuity equation is automatically satisfied. A Galerkin projection[3] of the momentum equations and the energy equation is then realized respectively onto the POD modes $\boldsymbol{\Phi}^u$ and Φ^θ. The reduced-order model is thus :

$$\begin{aligned}\frac{da_i}{dt} &= \sum_{j=1}^{N^u}\sum_{k=1}^{N^u} C_{ijk}\,a_j\,a_k + \sum_{j=1}^{N^u}\left(D_{ij}(\alpha,\sigma)+A_{ij}\right)\,a_j \\ &+ \sum_{j=1}^{N^\theta} B_{ij}\,b_j + E_{i1}(\alpha,\sigma) + E_{i2}(\alpha,\sigma) \\ &+ E_{i3}(\alpha,\sigma) + E_{i4}(\alpha,\sigma) \\ &\qquad\qquad \text{for } i=1,\ \ldots,\ N^u\end{aligned} \tag{10}$$

$$\begin{aligned}\frac{db_i}{dt} &= \sum_{j=1}^{N^u}\sum_{k=1}^{N^\theta} C^\theta_{ijk}\,a_j\,b_k + \sum_{j=1}^{N^\theta}\left(D^\theta_{ij}(\alpha,\sigma)+B^\theta_{ij}\right)\,b_j \\ &+ \sum_{j=1}^{N^u} A^\theta_{ij}(\alpha,\sigma)\,a_j + E^\theta_{i1}(\alpha,\sigma) + E^\theta_{i2}(\alpha,\sigma) \\ &\qquad\qquad \text{for } i=1,\ \ldots,\ N^\theta\end{aligned} \tag{11}$$

where the dynamical coefficients[4] depend on POD modes and mean fields which depend on control parameters. Indeed, each mean field $\bar{\mathbf{u}}(\mathbf{x},\boldsymbol{\alpha},\boldsymbol{\sigma})$ or $\bar{\theta}(\mathbf{x},\boldsymbol{\alpha},\boldsymbol{\sigma})$ is obtained by Lagrange interpolation, using the sampling (resp. $\bar{\mathbf{u}}(\mathbf{x},\boldsymbol{\alpha}_{\mathrm{POD}},\boldsymbol{\sigma}_{\mathrm{POD}})$ and $\bar{\theta}(\mathbf{x},\boldsymbol{\alpha}_{\mathrm{POD}},\boldsymbol{\sigma}_{\mathrm{POD}})$).

The reduced order model (Eqns. 10 and 11) corresponds to the constraint equations of the optimization problem (first variation of Lagrange functional $\mathcal{L}$ according to the adjoint variables $\boldsymbol{\xi}$ and $\boldsymbol{\zeta}$).

The reduced-adjoint equations

The variation of Lagrange functional $\mathcal{L}$ according to the state variables $\mathbf{a}$ and $\mathbf{b}$ yields the adjoint equations:

$$\begin{aligned}-\frac{d\xi_i}{dt} &= \sum_{j=1}^{N^u}\sum_{k=1}^{N^u}\left(C_{jik}+C_{jki}\right)\,a_k\,\xi_j \\ &+ \sum_{j=1}^{N^u}\left(D_{ji}(\alpha,\sigma)+A_{ji}\right)\,\xi_j \\ &+ \sum_{j=1}^{N^\theta}\sum_{k=1}^{N^\theta} C^\theta_{jik}\,\zeta_j\,b_k + \sum_{j=1}^{N^u} A^\theta_{ji}(\alpha,\sigma)\,\zeta_j \\ &\qquad\qquad \text{for } i=1,\ldots,N^u\end{aligned} \tag{12}$$

$$\begin{aligned}-\frac{d\zeta_i}{dt} &= \sum_{j=1}^{N^u}\sum_{k=1}^{N^\theta} C^\theta_{kji}\,a_j\,\zeta_k \\ &+ \sum_{j=1}^{N^\theta}\left(D^\theta_{ji}(\alpha,\sigma)+B^\theta_{ji}\right)\,\zeta_j \\ &+ \sum_{j=1}^{N^u} B_{ji}\,\xi_j + (b_i-\hat{b}_i) \\ &\qquad\qquad \text{for } i=1,\ldots,N^\theta\end{aligned} \tag{13}$$

with the terminal conditions:

$$\begin{aligned}\xi_i(T,\alpha,\sigma) &= 0, \\ \zeta_i(T,\alpha,\sigma) &= b_i(T,\alpha,\sigma)-\hat{b}_i(T,\alpha,\sigma)\end{aligned} \tag{14}$$

The optimality condition

Then, the optimality condition is obtained by deriving the Lagrange functional (Eqn. 9) according to the control variables α and σ. The resulting equations corresponds to the gradient expression of the cost functional according to α and σ : $\nabla_\alpha\mathcal{J}$ and $\nabla_\sigma\mathcal{J}$. We can deduce so the descent directions $d_{k1}=-\nabla_\alpha\mathcal{J}$ and $d_{k2}=-\nabla_\sigma\mathcal{J}$.

Summary

The constraints equations (Eqns. 10 and 11), the adjoint-equations (Eqns. 12 and 13) and the expressions of the gradient expression of the cost functional according to α and σ constitute the *optimality system*. It is solved here iteratively with this algorithm:

[3]Other projection methods can be also used, see for example Tallet et al. (2012).
[4]They are detailed in Tallet (2013).

1. Initialization: $k = 0$, $\alpha_k = \alpha_{ini}$ and $\sigma_k = \sigma_{ini}$
2. Known α_k and σ_k, solve the constraint equations (Eqns.10 and 11)
   $\rightarrow \mathbf{a}_k$ and $\mathbf{b}_k$
3. Known α_k, σ_k and $\mathbf{a}_k$, $\mathbf{b}_k$, solve the adjoint-equations (Eqns. 12 and 13)
   $\rightarrow \boldsymbol{\xi}_k$ and $\boldsymbol{\zeta}_k$
4. Estimate the descent directions with optimality conditions
   $\rightarrow d_{k1} = -\nabla_\alpha \mathcal{J}_k$
   $\rightarrow d_{k2} = -\nabla_\sigma \mathcal{J}_k$
5. Evaluate the new optimality parameters
   $\rightarrow \alpha_{k+1} = \alpha_k + w_{k1} d_{k1}$
   $\rightarrow \sigma_{k+1} = \sigma_k + w_{k2} d_{k2}$
   where the two steps w_{k1} and w_{k2} are determined by linear search.
6. Estimate convergence criteria ($\|\nabla_\alpha \mathcal{J}\| < \varepsilon_1$ and $\|\nabla_\sigma \mathcal{J}\| < \varepsilon_2$).
   If convergence criteria are unsatisfied, back to step 2.

1.2 Second method

The previous approach is efficient and very fast but can be costly in memory storage, whereas the current controllers are limited in space of storage. In this communication, we propose a second method, always based on POD decomposition, but without dynamical systems. Nevertheless, this method is less accurate, as only the mean field of velocity and temperature are considered, when the flow is established.

This second method, using the current controllers, enables to evaluate the temperature in the comfort zone. It will be sufficient then just add it in numerical controllers.

The first step is offline (outside the control loop) and the second step is online (in the control loop). They are described in the next subsections.

Offline

First, the velocity and temperature mean fields are decomposed by POD, using simulations with several values of inlet airflow rate q_v and inlet air temperature θ_{ext}, such as:

$$\mathbf{u}(q_v^{\text{data}}, \theta_{\text{ext}}^{\text{data}}, \mathbf{x}) = \sum_{i=1}^{N^u} a_i^u(q_v^{\text{data}}, \theta_{\text{ext}}^{\text{data}})\, \boldsymbol{\Phi}_i^u(\mathbf{x}) \quad (15)$$

$$\theta(q_v^{\text{data}}, \theta_{\text{ext}}^{\text{data}}, \mathbf{x}) = \sum_{i=1}^{N^\theta} a_i^\theta(q_v^{\text{data}}, \theta_{\text{ext}}^{\text{data}})\, \Phi_i^\theta(\mathbf{x}) \quad (16)$$

Only the data $a_i^u(q_v^{\text{data}}, \theta_{\text{ext}}^{\text{data}})$, $a_i^\theta(q_v^{\text{data}}, \theta_{\text{ext}}^{\text{data}})$, $\boldsymbol{\Phi}_i^u(\mathbf{x}_{\text{mes}})$ and $\Phi_i^\theta(\mathbf{x}_{\text{mes}})$, $\boldsymbol{\Phi}_i^u(\mathbf{x}_{\text{zone}})$ and $\Phi_i^\theta(\mathbf{x}_{\text{zone}})$ are boarded into the controllers. The points $\mathbf{x}_{\text{mes}}$ and $\mathbf{x}_{\text{zone}}$ correspond to the points at the measured temperature at the walls (sensors position) and the occupation (or comfort) zone[5]. The memory storage is thus considerably decreases.
This step can be costly in CPU time (simulations, POD bases construction) is realized once before the control loop.

Online

The next steps constitute the loop control:

1. Measure of the temperature at the walls $\theta_{\text{mes}}(\mathbf{x}_{\text{mes}})$.
2. Measure of the temperature at the room inlet θ_{ext}.
3. Evaluate the inlet airflow rate q_v (unknown), by using an optimization algorithm. The optimization problem considered here is to seek the inlet airflow rate (and knowing the inlet temperature θ_{ext}) corresponding to the "measured" temperature at the sensors $\theta_{\text{mes}}(\mathbf{x}_{\text{mes}})$ such that the next functional is minimized in the least squares sense:

   $$\mathcal{J}(q_v, \theta_{\text{ext}}, \mathbf{x}_{\text{mes}}) = \frac{1}{2} \sum_{j=1}^{M} \left(\theta_{\text{mes}}(\mathbf{x}_{\text{mes},j}) - \sum_{i=1}^{N_\theta} a_i^\theta(q_v, \theta_{\text{ext}})\, \Phi_i^\theta(\mathbf{x}_{\text{mes},j}) \right)^2 \quad (17)$$

   where M is the number of sensors.
   It is solved with the second-order descent algorithm.
4. Estimate the temperature in the comfort zone $\mathbf{x}_{\text{zone}}$ with the inlet air velocity, using the equation (Eqn. 18). Indeed, once the inlet airflow rate q_v obtained and knowing the inlet temperature θ_{ext}, the temperature in the occupation zone θ_{zone} and the velocity $\mathbf{u}_{\text{zone}}$ are determined by POD reconstruction as:

   $$\theta_{\text{zone}}(\mathbf{x}_{\text{zone}}) = \sum_{i=1}^{N^\theta} a_i^\theta(q_v, \theta_{\text{ext}})\, \Phi_i^\theta(\mathbf{x}_{\text{zone}}) \quad (18)$$

   $$\mathbf{u}_{\text{zone}}(\mathbf{x}_{\text{zone}}) = \sum_{i=1}^{N^\theta} a_i^u(q_v, \theta_{\text{ext}})\, \Phi_i^u(\mathbf{x}_{\text{zone}}) \quad (19)$$
5. Modify the inlet airflow rate q_v in order to achieve the target temperature (fixed by the occupant).

The last step is not presented here, only the methodology is tested.

[5] The position of the sensors and the occupation zone are determined before the control loop by the programmer.

RESULTS AND DISCUSSION

Both methods are compared onto the case of a lid-driven cavity heated by the left. Then, the second method is applied on the 3D-ventilated cavity, close to the real conditions of the building naturally ventilated.

2.1 Lid-driven cavity heated by the left

The fluid flow is in a lid-driven square cavity driven by the top with an intensity U_0, see Fig. (1). A hot and cold temperature are respectively imposed on the left and right walls and the others walls are taken adiabatic. The fluid is initially at rest. The air flow is incompressible, in the volume Ω of length H with boundaries Γ. The fluid dynamics is assumed governed by the Navier-Stokes equations and the temperature field by a convection-diffusion equation which are previously described (Eqn. 3).

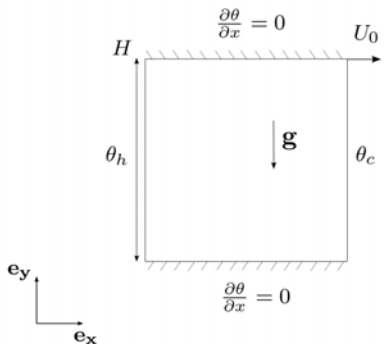

Figure 1: Geometry of studied cavity

In this case, we search to control the temperature field by adjusting the lid velocity defined such as : $\mathbf{u}_{|\Gamma_{top}} = \alpha\, U_0\, \mathbf{e_x}$ and the hot temperature : $\theta_{|\Gamma_{left}} = \sigma\theta_h$. The database, required to compute the POD bases, is constituted by using 3 values of α associated with 2 values of σ. The corresponding Reynolds, Grashof and Richardson number ($Ri = Gr/Re^2$) are listed in the Table 1.

Table 1: Dimensionless numbers composing the POD bases.

Reynolds *Re*	**Grashof** *Gr*	**Richardson** *Ri*
158	1.10^6	40
	5.10^6	200
316	1.10^6	10
	5.10^6	50
474	1.10^6	4
	5.10^6	22

All this flows are computed by *Code_Saturne*[6] from $t = 0$ to $t = 15$, using a mesh 100×100.

2.1.1 First method

Thirty velocity and sixteen temperature POD modes are kept to build the reduced-order model (Eqns. 10 and 11).

Control loop

The optimization problem previously described is now considered. The constraints equations (Eqns. 10 and 11), the adjoint-equations (Eqns. 12 and 13) and the expressions of the gradient expression of the cost functional according to *Re* and *Gr* constitute the *optimality system*. Initializing the algorithm with values different from the target, the goal is to reach the wished target. Four target parameters are tested, using the following values of dimensionless numbers (which do not belong to the sampling):

- $Re_{\text{tar1}} = 221$; $Gr_{\text{tar1}} = 2.10^6$ ($Ri_{\text{tar1}} = 41$)
- $Re_{\text{tar2}} = 221$; $Gr_{\text{tar2}} = 4.10^6$ ($Ri_{\text{tar2}} = 82$)
- $Re_{\text{tar3}} = 379$; $Gr_{\text{tar3}} = 2.10^6$ ($Ri_{\text{tar3}} = 14$)
- $Re_{\text{tar4}} = 379$; $Gr_{\text{tar4}} = 4.10^6$ ($Ri_{\text{tar4}} = 28$)

The control algorithm converges quickly (around two minutes on a cluster against several hours on twenty four clusters with the full model) towards the target in about twenty iterations, see Figures 2 and 3.

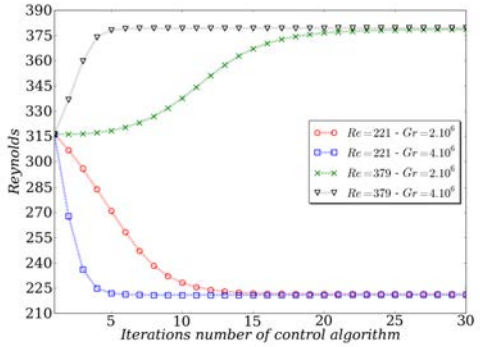

Figure 2: Convergence of control algorithm, according to the parameters control (Reynolds number).

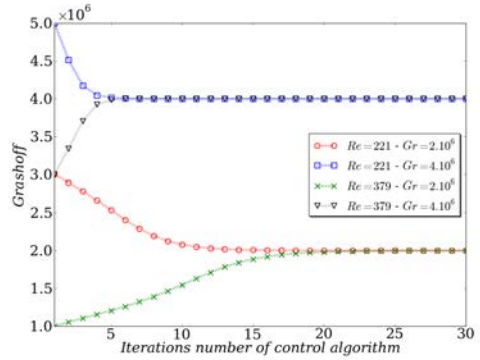

Figure 3: Convergence of control algorithm, according to the parameters control (Grashof number).

[6] *Code_Saturne* is an open source CFD software, developed by EDF Research.

Reduced-order model

The relevance of our model is now tested. For this, we use the following values of dimensionless numbers, which do not belong to the sampling :

1. $Re = 221$; $Gr = 2.10^6$ ($Ri = 41$)
2. $Re = 221$; $Gr = 4.10^6$ ($Ri = 82$)
3. $Re = 379$; $Gr = 2.10^6$ ($Ri = 14$)
4. $Re = 379$; $Gr = 4.10^6$ ($Ri = 28$)

The time-average error[7] between the full model and the reduced model is listed for each case on the Table 2. The obtained results are accurate (error below to 10%), the reduced-order model developed here enables to reproduce a flow at the dimensionless number different to those of the sampling.

Table 2: Time-average error between the fields obtained with the full model and the reduced-order model.

case	temperature	velocity
1	5,15 %	11,7 %
2	4,74 %	13,8 %
3	5,78 %	10,8 %
4	5,47 %	13,6 %

Nevertheless and as mentioned in the methodology section, this model is too costly in memory storage. For example, in the case of lid-driven cavity, it would boarding on the controllers around 30Mo of data. In the real case, the POD modes number is higher, the cost due to storage would be even more important.

2.1.2 Second method

This same case has also dealt in using the second method. The database is constituted of the same sample that previously (Table 1), but the velocity and temperature fields are now averaged in time. Three velocity and temperature POD modes are here kept. The same target values of dimensionless numbers are considered.

Three sensors have been necessary and the occupation zone has been determined as shown on Figure 4.

The optimization algorithm is very quickly ($<$ 3s) and the results are rather satisfying (see Table 3). Indeed, the mean error in the occupation zone between the fields obtained with the full model and the reduced approach are less than 8%. Moreover with this method, only 1Mo of data have to be boarded. But, it is to be noticed that the second method enables to obtain only the mean fields.

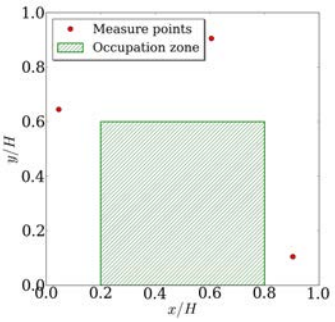

Figure 4: Position of the sensors and occupation zone in the lid-driven cavity.

Table 3: Mean error in the occupation zone between the fields obtained with the full model and the reduced approach, for each considered case.

case	temperature	velocity
1	1,27 %	8,03 %
2	0,40 %	6,33 %
3	1,50 %	7,53 %
4	0,41 %	7,19 %

2.2 3D ventilated cavity

The fluid flow is in a cubic fluid domain Ω of dimensions $L \times H \times P$ and boundaries Γ with an inlet and an outlet, see Fig. 5. The air fluid intensity on the inlet Γ_{in}, located at a distance 0.1 from the bottom is imposed to U_0 and an condition outlet is fixed on outlet Γ_{out} at a distance 0.2 from the top of the cavity. A temperature $\theta_w = 27°C$ is imposed on all walls, except to the right wall where the temperature is hotter ($\theta_h = 30°C$). The inlet air temperature θ_{ext} is colder, in order to refresh the cavity.

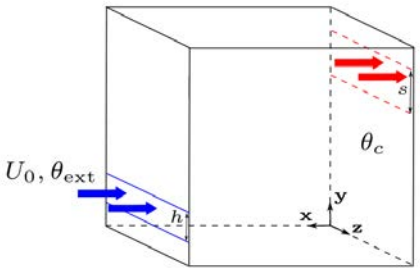

Figure 5: Geometry and boundaries conditions of the ventilated cavity.

In this case, the goal is to control the temperature, by adjusting the inlet air velocity[8]. In order

[7] The time-average error is defined such as : $\text{e}(\%) = \int_0^T \frac{|f_{full}(t) - f_{ROM}(t)|_{L_2}}{|f_{full}(t)|_{L_2}}\, dt$.

[8] Here, we considerer that the inlet airflow rate is related to the inlet air velocity.

to validate our methodology (second method), we search here to find the temperature into the occupation zone, using the available data which are measured by the sensors in the cavity: the temperature at the walls and the inlet air temperature.

The Figure 6 represents the four sensors at the walls and the occupation zone in the 3D ventilated cavity.

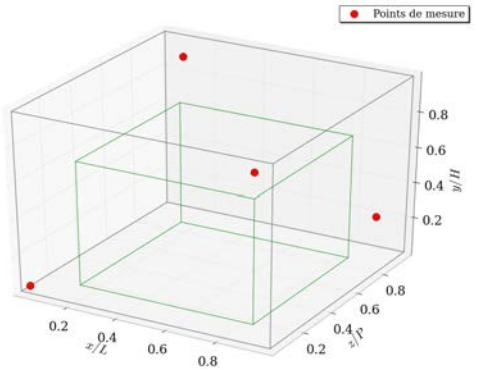

Figure 6: Sensors position (red circles) and occupation zone (green cube) in the cavity (grey cube).

The first step consists in building the database with full simulations. For this, we use the values of the inlet air velocity and temperature listed on the Table 4. The POD bases are then built, using the equations (Eqns. 15 and 16). In the following, five velocity and temperature POD modes are kept.

Table 4: Values of the inlet air velocity and temperature belonging to the database

Inlet air velocity U_0^{data} $(m.s^{-1})$	**Inlet air temperature** $\theta_{\text{ext}}^{\text{data}}$ (°C)
0,2	14; 18; 22
0,4	14; 18; 22
0,6	14; 18; 22
0,8	14; 18; 22
1,0	14; 18; 22

The goal is to reach values of inlet air velocity U_o and temperature θ_{ext}, which do not belong to the sampling. Four cases have been tested:

1. $U_0 = 0,70 m.s^{-1}$; $\theta_{\text{ext}} = 16$°C
2. $U_0 = 0,50 m.s^{-1}$; $\theta_{\text{ext}} = 20$°C
3. $U_0 = 0,90 m.s^{-1}$; $\theta_{\text{ext}} = 21$°C
4. $U_0 = 0,30 m.s^{-1}$; $\theta_{\text{ext}} = 15$°C

After estimating the inlet air velocity U_o with an optimization algorithm, the fields in the occupation zone are obtained, according to the equations (Eqns. 18 and 19).

The optimization algorithm is very fast ($< 10s$). The average-space error for temperature is less than 0,1% and for the velocity around 25% (Table 5). The isocontours of temperature are represented on the Figure 7 for each model. Our model enables to reproduce the flow with accuracy, the difference between the temperature obtained with the full model and the reduced approach below to 1°C. This results are rather satisfying and this method should now be implemented in current controllers in real conditions.

Table 5: Average-space error between the fields obtained with the full model and the reduced approach in the occupation zone

case	**temperature**	**velocity**
1	0,12 %	17,96 %
2	0,09 %	26,36 %
3	0,08 %	21,40 %
4	0,10 %	37,23 %

CONCLUSION

In this paper, two methods have been presented in the order to control in real-time the indoor airflow in the buildings. These are compared on the case of a lid-driven cavity heated by the left.

The first method enables to control the temperature field quickly ($\approx 1,2$ min) and to obtain the temporal evolution of the velocity and temperature, with a good accuracy (error $< 14\%$). However to be integrated into existing controllers, this method requires again too storage space (of the order of tens of Mo).

That is why only the second method has been applied on a 3D ventilated cavity, similar to a room naturally ventilated. This method is efficient, requires less storage of data and very fast (a few seconds). It would be enough simply to add in the programming of current controllers, the step of estimating the inlet air velocity (or airflow rate in practice) and the step of determining the temperature in the occupation zone.
Monitoring would be performed either on the measured temperature to the walls, but on the temperature in the occupation zone, which facilitate the study of acceptable conditions of thermal comfort to occupants.

ACKNOWLEDGEMENT

The authors gratefully acknowledge the financial supports provided by the Agence Nationale de la Recherche (ANR-08-HABISOL-019).

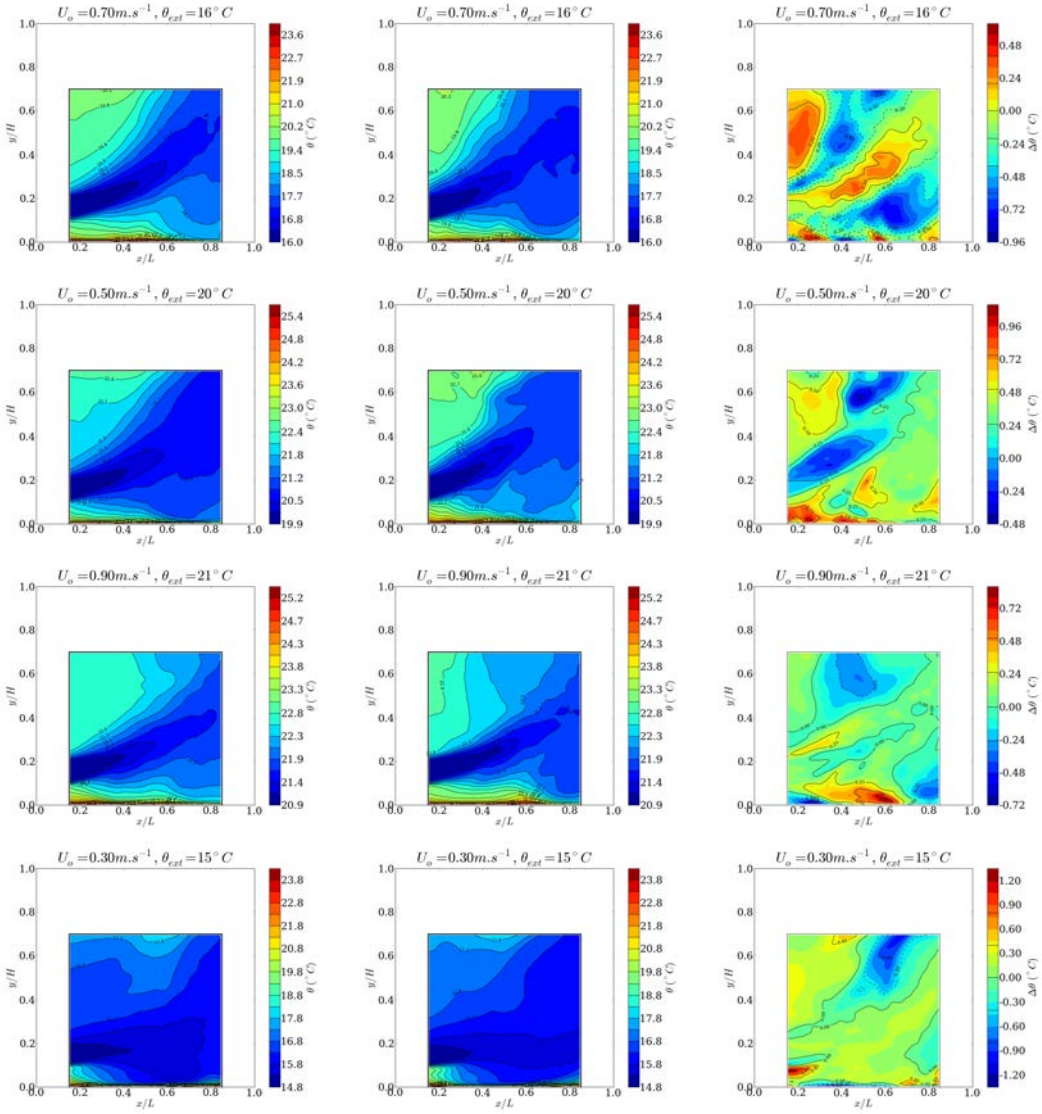

Figure 7: Isocontours of temperature in the occupation zone at $z/P = 0.5$.

Bibliography

Bergmann, M. and Cordier, L. 2008. Optimal control of the cylinder wake in the laminar regime by trust-region methods and POD reduced-order models. *J. of Comp. Phys.*, 227(16):7813–7840.

Gunzburger, M. D. 2003. *Perspectives in Flow Control and Optimization*. Advanced in Design and Control, SIAM.

Palomo Del Barrio, E., Lefebvre, G., Behar, P., and Bailly, N. 2000. Using model size reduction techniques for thermal control applications in buildings. *Energy and Buildings*, 33(1):1–14.

Ravindran, S. 2000. Reduced-order adaptive controllers for fluid flows using POD. *J. of Scientific Computing*, 15:457–478.

Sempey, A., Inard, C., Ghiaus, C., and Allery, C. 2009. Fast simulation of temperature distribution in air conditioned rooms by using proper orthogonal decomposition. *Building and Environment*, 44:280–289.

Tallet, A. 2013. *Contrôle des écoulements par modèles d'ordre réduit, en vue de l'application à la ventilation naturelle des bâtiments*. PhD thesis, Université de La Rochelle.

Tallet, A., Leblond, C., and Allery, C. 2012. Anisothermal flow control by using reduced-order models. *ASME 2012, 11th Biennial Conference On Engineering Systems Design And Analysis, Nantes, France*.